J. J. McCann,
"Color Gamut Measurements and Mapping:
The Role of Color Spaces",

in Color Imaging: Device independent Color, Color Hardcopy,
and Graphic Arts IV,

G. Beretta and R. Eschbach, eds.

Proc. SPIE, **3648**, 68-82, 1999.

Invited Paper

Color Gamut Measurements and Mapping: The Role of Color Spaces.

John J. McCann
McCann Imaging, Belmont, MA 02478
mccanns@tiac.net

ABSTRACT

Before embarking on an extensive set of color gamut mapping experiments, we were distracted by wanting to understand uniform color spaces. The CIE L*a*b* is almost universally used for a Colorimetric Uniform Color Space. It is found most often in the literature and is used by many instrument makers as Colorimetric output. There are a wide variety of papers that imply small errors in L*a*b*. Nevertheless, the sense of these articles is that the errors are small local perturbations about an average response that is essentially correct. Many papers describe small improvements using modified equations.

This paper will present measurements and literature data that show surprisingly large discrepancies between CIE La*b* and isotropic observation-based Color Spaces such as Munsell.

- CIE L*a*b* exaggerates chroma particularly at high saturations
- The average discrepancy between L*a*b* and an ideal isotropic rendering for all Munsell chips is 27% [delta E = 8±6]
- Munsell's equally spaced hue angles are distorted up to 20 degrees by L*a*b*
- Chips with identical L*a*b* hue angles do not appear the same color

Clearly, L*a*b* will introduce errors as large as the gamut-matching problem under consideration. A better solution needs to be found to do gamut mapping studies.

We have ideal data in the Munsell Book. We used the original renotation published by Newhall, Nickerson and Judd. Printed tables and approximation formulas were the only reasonable tools when the work on L*a*b* started decades ago. Today's computer systems allow 3-D lookup tables to convert instantly any measured L*a*b* to interpolated values scaled by the Munsell Book. We called this new space ML, Ma, Mb in honor of Munsell. This MLUT procedure reduces the isotropic error introduced by L*a*b* to zero for all Munsell chips. LUTs have been developed for both **LabtoMLab** and **MLabtoLab.** With this zero-error, isotropic space we can return our attention to the original problem of color-gamut image processing.

Keywords: Color spaces, color gamut, gamut mapping, Munsell, LAB, uniform color space.

INTRODUCTION

There is considerable interest in color matching between monitors and printers. The problem is well documented. The color gamut of the print is very different from that of the monitor. The monitor has a wide variety of different, highly saturated, high-value colors near white. Prints, even those using high extinction coefficient dyes, absorb too much light to generate these colors. Prints, however, have a bigger range of colors in the low-lightness browns. The hope is to find automatic calculations of monitor and print colors that make them look more like each other. Before embarking on quantitative evaluations of these ideas, we felt it necessary to study the color spaces used in automatic calculations. The ideal 3-D color space is isotropic. Namely, it has the same properties in all directions, for all parts of the space.

The cornerstone of colorimetry is the X,Y,Z three dimensional space. It is derived from color matching experiments and can predict if two samples, will match, based on full-spectrum measurements. Independent of X,Y,Z's ability to predict matches, it is not isotropic[1] and it cannot predict the sample's color appearance[2].

We are looking for a practical computational space that is has the same properties in all directions, for all parts of the space. Any two sample that are ***n*** units apart in a **uniform color space** will appear equally different whether the separation is in hue, lightness or chroma or a combination.

Part of the IS&T/SPIE Conference on Color Imaging: Device-Independent Color, Color Hardcopy, and Graphic Arts IV • San Jose, California • January 1999
SPIE Vol. 3648 • 0277-786X/98/$10.00

Observations vs. Equations

There are two different approaches to uniform color spaces. The first is observation. Munsell, OSA Uniform Color space and NCS are all examples of extensive research using human observers to select color samples that uniformly spaced. CIEL*a*b*, CIELuv, CIECAM97 are examples of mathematical functions that approximate the observer data. In this paper we will limit our discussion to Munsell observations and CIEL*a*b* calculations. Ideally the differences between the observed data and their calculated approximations are vanishingly small.

The advantage of the Munsell Book is that one can see the chips and evaluate for oneself how uniform it appears (Figure 1).

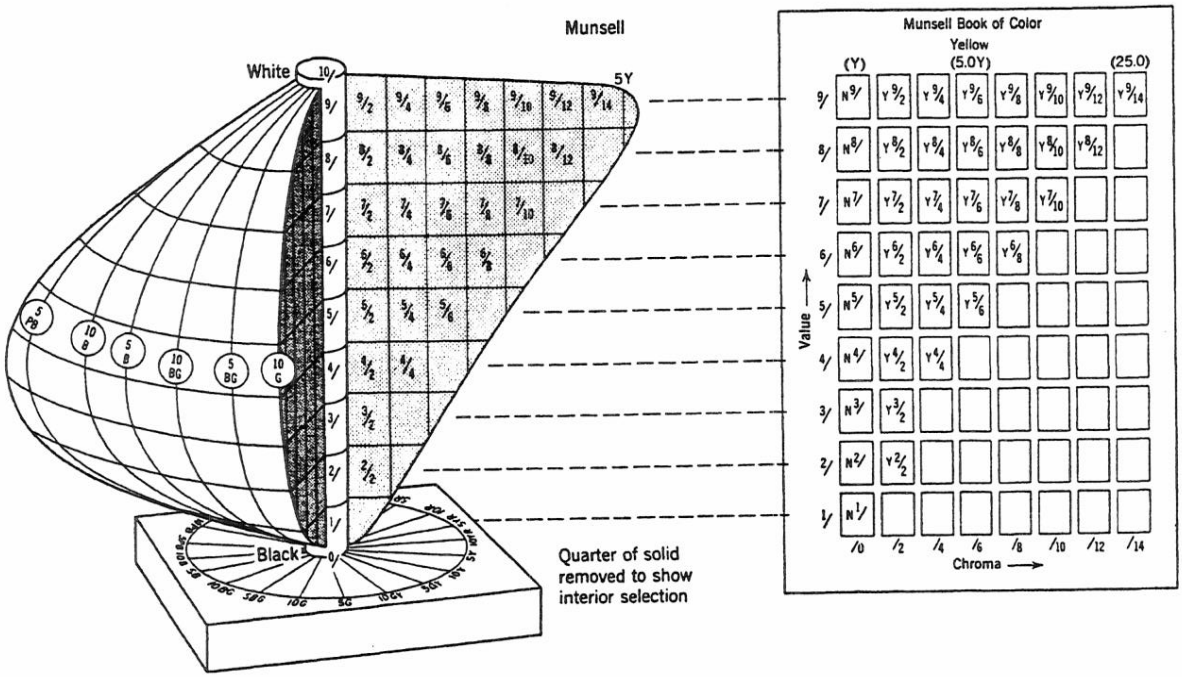

Figure 1 shows Nickerson's[3] diagram of the Munsell space. There are 40 planes of hues that share the neutral gray axis at the center. In each hue plane lightness and chroma are equally spaced.

The advantage of CIE L*a*b* is that it has become an almost universal standard in imaging. It is built into many measuring devices for direct measurements and it uses only three equations to calculate L*, a*, b* from X,Y,Z.

$$L^* = 116 * (Y/Y_n)^{1/3} - 16$$
$$a^* = 500 * [(X/X_n)^{1/3} - (Y/Y_n)^{1/3}]$$
$$b^* = 500 * [(Y/Y_n)^{1/3} - (Z/Z_n)^{1/3}]$$

HOW UNIFORM IS L*a*b* ?

A great many authors use CIE L*a*b* as the space of choice for making decisions on the best color compromise, such as the mapping of extra-gamut points in printed and displayed images. They select CIE L*a*b* because hue, lightness and chroma are approximately uniformly spaced. Before doing an extensive set of these so called gamut mapping experiments, we became curious about the actual size of CIE L*a*b*'s nonuniformities. There is an abundant literature that straddles the line between *it "does a respectable job"*[4] and *it needs improvement,* usually with more clever functions[5]. The following comparisons of Munsell observations and CIE L*a*b* calculations are an attempt to resolve this confusion.

Let us define a new space called MLab. M is in honor of Munsell. The idea is to mimic CIE L*a*b* format so we can easily compare the two. CIE L*a*b* Lightness varies from 100 to 0. Munsell notation varies from 9/ to 1/. By multiplying Munsell Lightness by 10, we closely approximate L*. By multiplying Munsell Chroma by 5 we approximate CIE L*a*b*'s Chroma.

A simple test is to look at the area of biggest concern in gamut mismatch, namely saturated yellows. A yellow Munsell 5.0 Y 8/14 has an expected MC value of 70 (14*5=70). However, when we measure the chip we get C*=103. L*a*b* has introduced an error of delta E = 33. CIE L*a*b* overestimates 5.0 Y 8/14's Chroma(MC) by (33/70=47%).

Another example is Munsell 10 B 6/8. Observers place the chroma at 40 (5*8=40). CIE L*a*b* places chroma at 31.9. L*a*b* has introduced an error of delta E = 8 CIE L*a*b* underestimates Munsell Chroma by 20% . These discrepancies between observation and calculation are much too large. If the entire CIE L*a*b* space has similar problems it should not be used in gamut mapping applications because the space will introduce errors that are very large.

Real Chips in the Munsell Book

The following study compares CIE L*a*b* values with the MLab values derived from Munsell Notation. The Data for CIE L*a*b* values come directly from Newhall Nickerson and Judd's 1943 paper[6] This familiar table[7] gives Y,x,y for 2742 chips. This set contains both 1317 real chip data and the remainder are defined by extrapolation to the spectrum locus.[8]

If we return for a moment to Figure 1, we can review the design of Munsell's Uniform Space.

- There are 9 horizontal Lightness planes perpendicular to the gray axis.
- There are concentric circles of chroma, with a gray at the center
- There are 40 hues that define vertical planes that are parallel to the gray axis down the center.
  - Each plane is made of colors with constant hue.
  - All hue planes are uniformly spaced (360/40=9 degrees apart)

The evaluation of the uniformity of CIE L*a*b* will be made on how well it portrays the fundamental design principles. Observers picked the Munsell papers using the above design criterion.

Figure 2 shows a plot CIE L*/C* values of all 1317 real chips in a Chroma vs. Lightness plane on the left. On the right is the plot of the same chips in MLab space. Here all colors fall on the equally spaced grid associated with Munsell Notaion. The CIE L*a*b* calculation shows excellent conformity in Lightness. All the data falls on parallel lines. It is the Chroma axis that fails to show uniform properties.

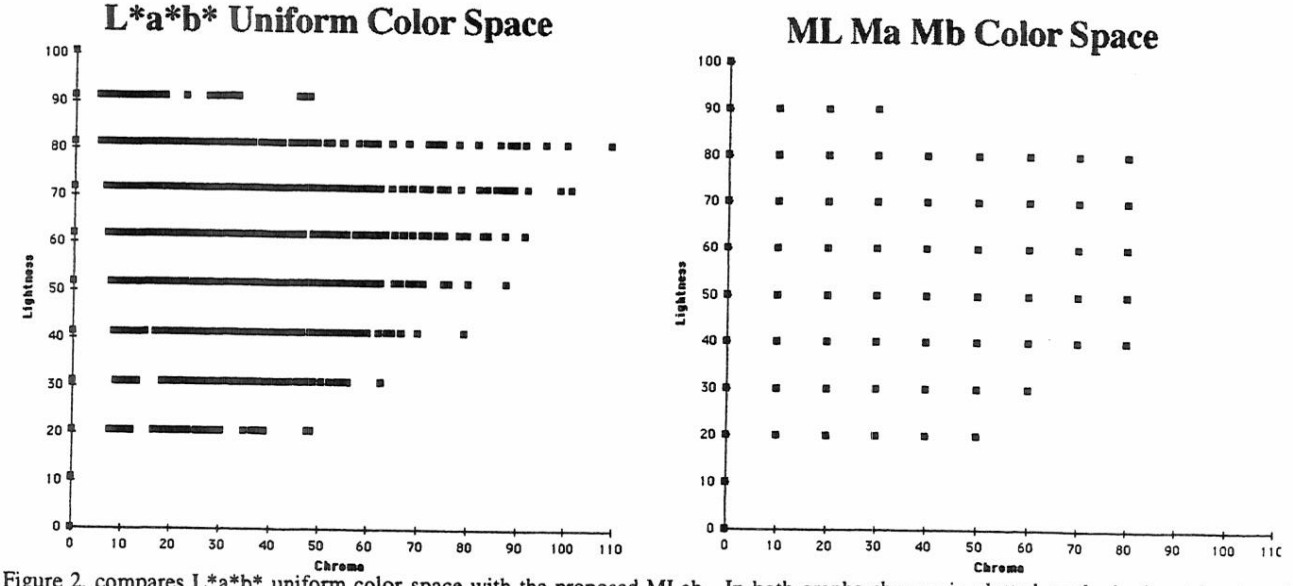

Figure 2. compares L*a*b* uniform color space with the proposed MLab. In both graphs chroma is plotted on the horizontal axis and lightness is plotted on the vertical axis. All hue planes are compressed into the L/C plane. L*a*b* is not uniform in Chroma.

Figure 3 plots the same data as Figure 2 in the a/b plane. Here all Lightnesses are compressed into a single plane. CIE L*a*b* is irregularly spaced. Some hues, such as yellow, expand the Chroma, others such as blues, compress the Chroma. The distinct radial lines created by Munsell have been blurred. The MLab plot on the right shows a regularly spaced array.

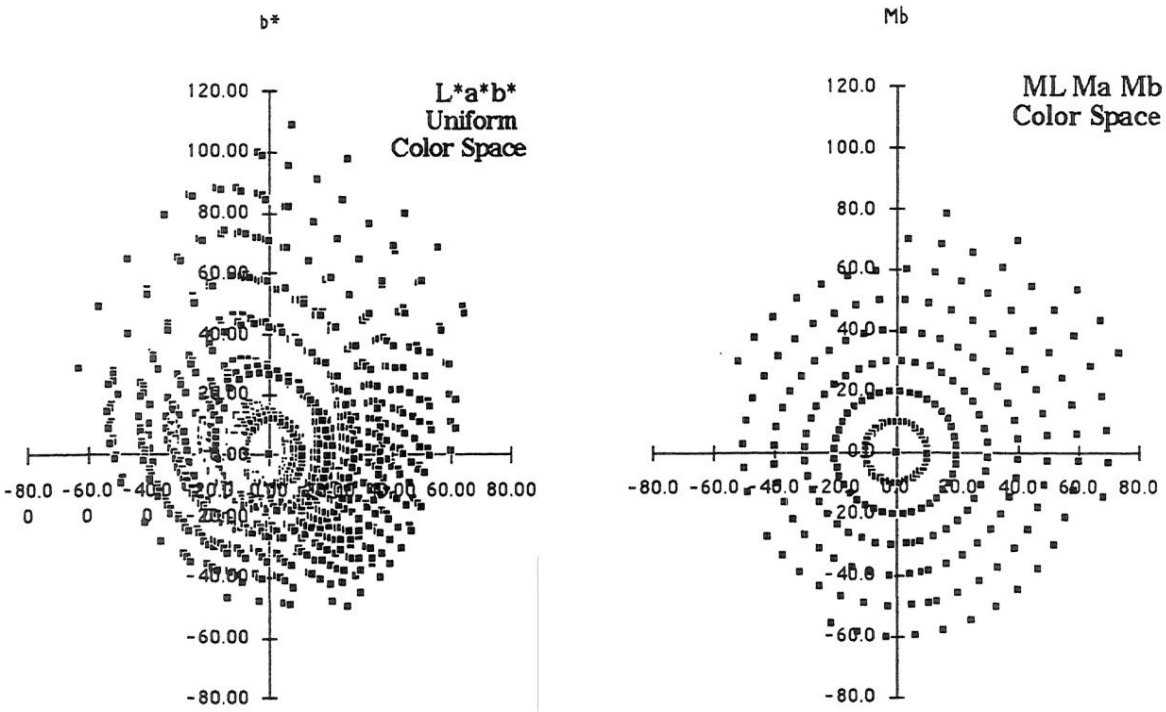

Figure 3. compares L*a*b* uniform color space with the proposed MLab. In both graphs a is plotted on the horizontal axis and b is plotted on the vertical axis. All lightness planes are compressed in the a/b plane. Again, L*a*b* is irregularly spaced.

The blur in hue angle observed above can be seen more clearly in Figure 4. Here we look at all the chips found on the 2.5 R, 5 R and 7.5 R pages. We plot the hue angle in CIE L*a*b* space on the vertical axis and give the name of the chip on the horizontal axis. Munsell Notation (MLab) places all 2.5 R hues on the solid line at 9 degrees, all 5 R chips on the 18 degrees line and all 7.5R chips on the 27 degree line. CIE L*a*b* portrays constant hues as drifting across three pages. The drift in Figure 3 is caused by the fact that CIE L*a*b* does not position chips with constant hue in a single vertical plane. It creates a slanted plane that undulates with chroma.

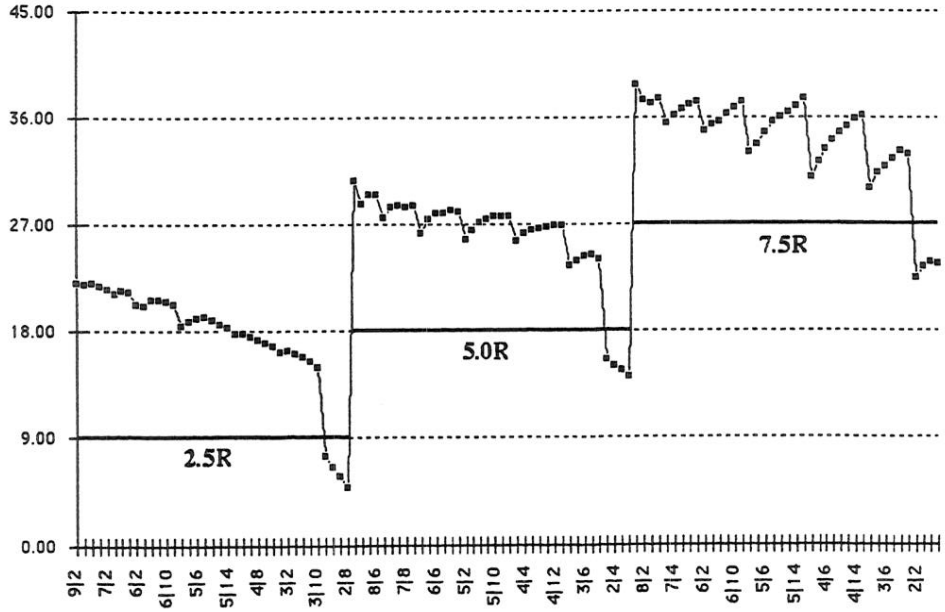

Figure 4 shows the plot of hue angle on the vertical axis vs. all the chips on three pages of the Munsell book. Ideally all the L*a*b* points should fall on the solid lines. A hue angle of 20 degrees could be a light 2.5R or a dark 5.0 or 7.5 R chip. CIE L*a*b* does not present the same hue in a plane parallel to the gray scale. Rather constant hue is a slanted, rippled surface.

We have defined the expected hue angle in MLab space by setting 10 RP to 0 degrees. Then, all 2.5R chips are at 9 degrees, all 5.0 R chips are at 18 degrees, ... and all 7.5 RP chips are at 351 degrees. We can measure the hue error by subtracting MLab hue angle from CIE L*a*b* hue angle . Figure 5 shows this error plotted on the vertical axis vs. all the real chips in the Munsell Book. Ideally, all the errors would fall close to the 0 line. The data, however, shows that there is considerable variability for each page in the book, as well as drift around the hue circle.

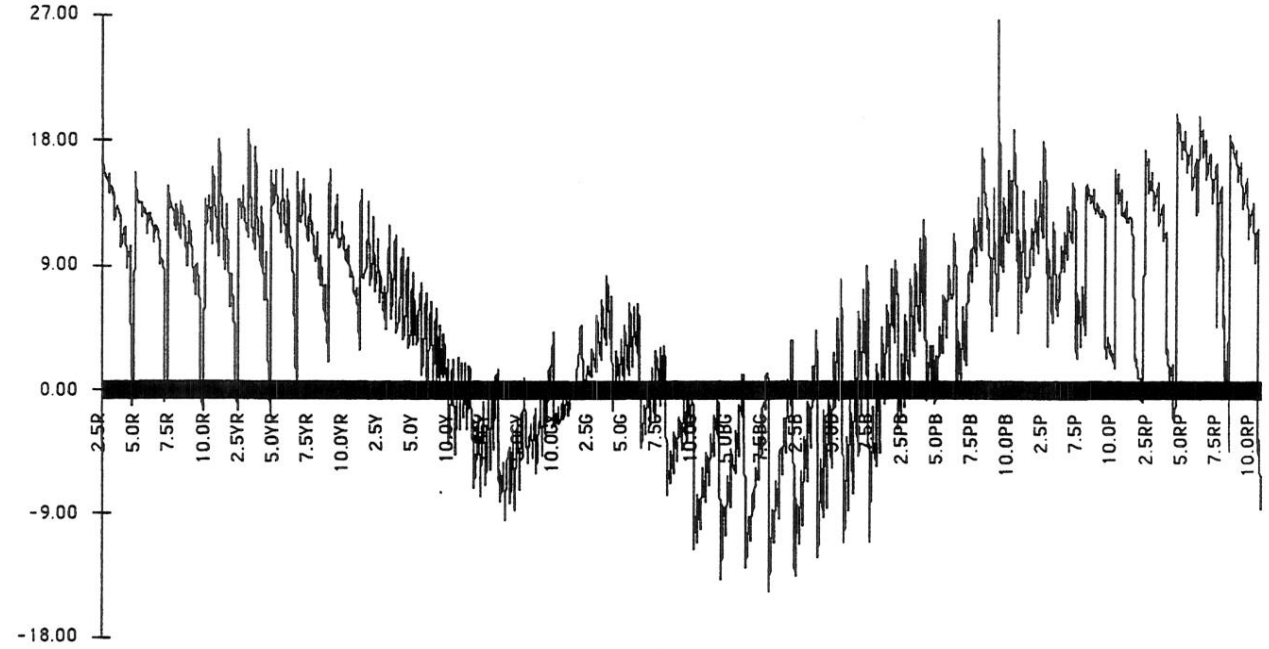

Figure 5 shows the error in hue angle introduced by CIE L*a*b*. The vertical axis is the [CIE L*a*b* hue angle - MLab hue angle]. The horizontal axis is all the real chips in the Munsell book.

In order to summarize the results so far, we can review the how CIE L*a*b*portrays the Munsell book.

- There are horizontal Lightness planes perpendicular to the gray axis. This is in excellent agreement with Munsell.
- There are irregular shapes instead of concentric circles of increasing chroma.
- The 40 hues are not vertical planes parallel to the gray axis.
  - Constant hues form a corrugated, slanted plane.
  - Hue planes are non-uniformly spaced

Except for Lightness, CIE L*a*b* distorts the fundamental design principles of the Munsell book. Since virtually all the errors are in the a/b planes we can evaluate the magnitude of the errors by measuring the distance between CIE L*a*b* position and the MLab position in the a/b plane.

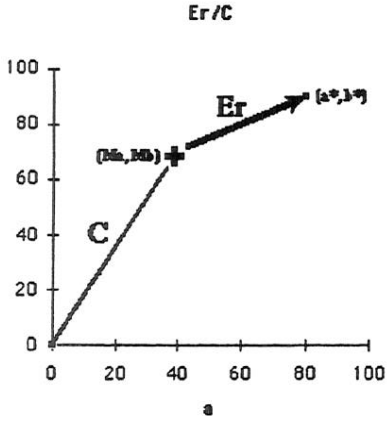

Figure 6 illustrates Er/C, used as a measure of error. The (Ma, Mb)coordinates show the location in MLab. The (a*, b*) coordinates show the location in CIE L*a*b*. The line C is the distance from the origin to (Ma, Mb). The line Er is the magnitude of the error introduced by CIE L*a*b*. It is the distance between (Ma, Mb) and (a*, b*). We evaluated each chip in the Munsell Book as a percentage error by the ratio of Er to C.

Figure 7 shows the histogram of E_r/C for all 1731 real chips in the Munsell book. The maximum error is 82%, the minimum is 0.01%, The mean is 27%; the standard deviation is 13% and the median is 24%.

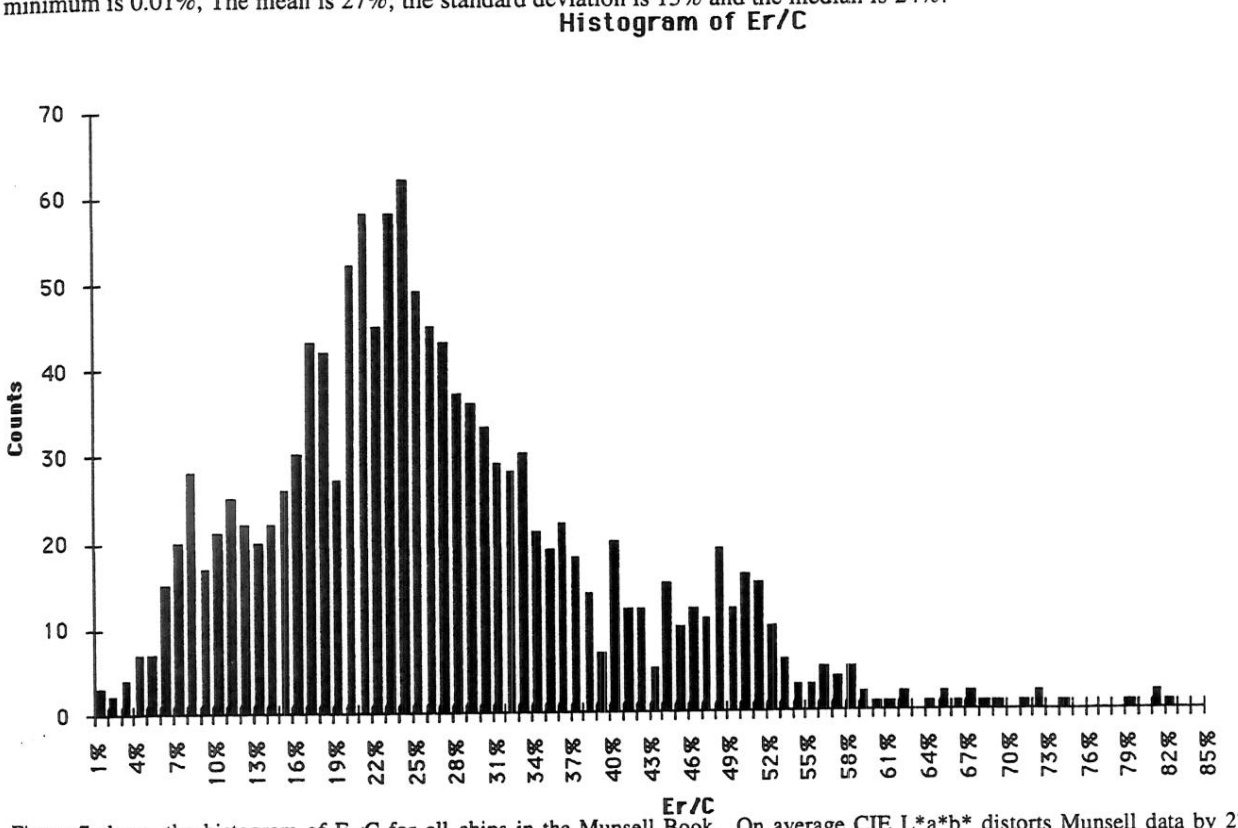

Figure 7 shows the histogram of E_r/C for all chips in the Munsell Book. On average CIE L*a*b* distorts Munsell data by 27% of Chroma.

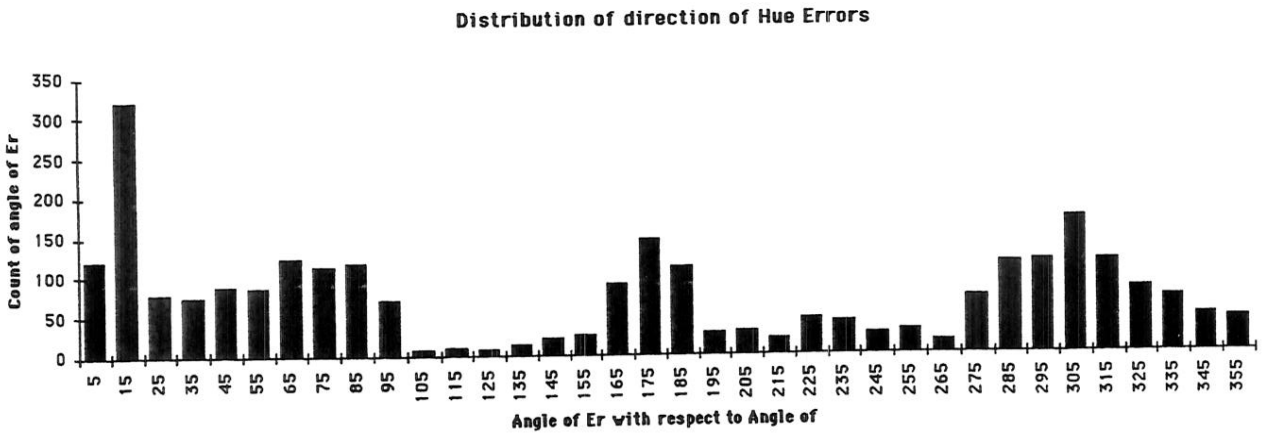

Figure 8 is a histogram of the angle of Er with respect to C. The demonstrates again that there is no apparent simple relationship between observed data (MLab) and calculations (L*a*b*).

Table 1 lists E_r and E_r/C for all the real chips in the Munsell Book. The rows report data for a particular Hue and Lightness. The columns report vales for different Chromas. Averages are presented at the end of the table.

APPROACHES TO FIX THE CIE L*A*B*'S PROBLEMS

Over the years since 1976 when L*a*b* became a CIE standard, there have been a number of papers discussing the problems and recommending improvements.[9] There are far too many to review in detail. Needless to say none of these improvements have enjoyed such common usage as CIE L*a*b*.

Find the 'magic bullet' function

The most frequently found approach has been to find mathematical functions that can fit the observer data better.[10] RLAB replaces the coefficients 500 and 200 with 430 and 170.[11] This makes the average error for all chips approach zero, but does little to improve the individual errors. The advantages of using equations is that they are easily to compute by hand, slide rule, or with a calculator. The disadvantage is that all of these functional approximations lack the precision necessary to render Munsell with vanishingly small errors. Munsell's entire color space is much more complex than the equations used to approximate it.

3D LUTs

In the 1980's the Polaroid Vision Research Laboratory began a series of experiments attempting to characterize the behavior of Polacolor instant film in devices that exposed the film using digital control of three narrow-band illuminants. Instant film has highly nonlinear properties. The three sets of dyes that form the final image are in a nine layer structure that also contains the three light-sensitive emulsions. First, the cyan dye has to migrate past the red-sensitive emulsion that controls its concentration in the final image. Then, it must pass through the magenta dye layer, the green sensitive emulsion, the yellow dye layer, the blue-sensitive emulsion and the viscous developer to reach the mordant layer. Obviously, the amount of cyan dye in the final image depended primarily on the red exposure, but it was significantly influenced by the green exposure and the blue exposures.

We studied the problem from two perspectives: mathematical models and 3-D LUTs. Although we were able to model the system with high order polynomials we found that process too slow and painful to apply to practical working environments. By using the inherent power of scanners and computers, we found it faster, simpler and easier to measure the response of a film to all possible combinations of the three exposures, than to accurately model its complete behavior. With a known digital image test target we exposed all combinations of 8 levels of R, G, B. Scanners read that image and programs selected the pixels associated with each test patch. This made sure that any error in alignment of the print was corrected.

The film's response in all parts of the color space was used to create any desired color. This system was used in a Color Transform Board designed by the Vision Research Lab that resided in the MacDonald Detweiller FIRE 300 film recorders. This device was an early digital prepress proof system. Starting with digits used to make the press plate, along with press calibrations, we calculated the desired color for each pixel. Using the calibrated response of the film we can calculate the three exposures to write, pixel by pixel, a highly accurate prepress proof. All image calculation were done by the 3-D hardware lookup table. The calibration of the press and the calibration film were combined so that there was only one operation performed in hardware Color Transformation board. This board resides in the printer. Digits used to make printing plates were sent to the film recorder. The color transform board stored map coefficients derived from the press and film calibrations. The input digits were sent to the look up table. All combinations of the most significant five digits were prestored in the board. Using prestored information from all nearest neighbors we interpolated the best output in the least significant bits. A more complete description can be found in a U.S.patent entitled *Method and Apparatus for Transforming Color Image Data on the Basis of an Isotropic and Uniform Colorimetric Space*[12]

Kotera and his colleagues[13] have used 3-D LUTs in a wide variety of applications, including high speed video applications.

The 3-D LUTs techniques is used to make accurate color reproductions of paintings[14]

Many commercial products use 3-D LUTs as the most efficient way to calculate accurate information in real time applications.

If we think of the Uniform Color Space problem as a candidate for 3-D LUTs we have:

Advantages

- All 1317 Munsell chips have zero error (they are table lookups)
- All intermediate values are computed from all their nearest neighbors.

Requirements

Requires a computer program and LUT

- Size of program = 80KB
- Size of LUT = 806KB
- Run time = 1 second for all 1317 chips in the Munsell book

Disadvantages

- Difficult to do with a slide rule
- There are no disadvantage for anyone using a computer.

The lookup table function has been possible for many years, first by using the Newhall Nickerson and Judd table as originally designed. The real-time conversion from Munsell Notation to L*a*b* and and the inverse interpolation can be done with a Munsell conversion program sold by Munsell of GraytagMacbeth. It can be found on the web at

http://munsell.com/Download.htm

Munsell notation is far from ideal in format. Lab 's format was chosen so that the one can calculate distances and angles. The ideal case is to use Munsell information to calculate a MLab space and use it as we would CIE L*a*b*. To be effective we need 3-D LUTs to convert LAB to MLAB and MLab to Lab.

A working MLab 3-D LUT

The best source of data for a 3-D LUT is the data from Newhall, Nickerson and Judd (NNJ). Here they list Munsell Notation colors that are uniformly spaced in appearance. The foundation is a very large study of real papers selected by extensive observer experiments. They interpolate colors out to the spectrum locus. They provide an atlas of all possible colors that are uniformly spaced.

First we need to make a 3-D table of equivalents. We used the (NNJ)Y,x,y data to calculate L*a*b* in 5000 degree Kelvin illumination for each chip. The MLab designation was calculated from Munsell notation as follows:

- Hue angle for 10 RP was set to 0 degrees.
- A Table of the 40 hue pages were spaced 9 degrees
  2.5R=9 degrees; 5.0R=18 degrees;... 7.5RP =351 degrees.
- H = Hue angle from the above table
- ML = 10*Value notation
- MC = 5* Chroma notation
- Ma = MC*cosH
- Mb = MC*sinH

With Gary Dispoto and Michael McGuire of HP labs we created a pair of 3D LUT **LabtoMLab** and **MLabtoLab** and two programs to use them. The input and output channels of the LUTs are scaled to 8-bits. The tables are 65x65x65x3 planes, 824k, which means the six most significant bits are looked up and the two least significant bits are interpolated. The programs do the transform in either direction, depending on the table used. One program makes single calculations, with input and output in normal units. The other program is for transforming TIFF images and uses the standard representation of L*a*b*. The programs are console applications for Win NT or WIN95/98.

All programs ran on an HP Kayak PC with a 300 MHz processor. The **LabtoMLab** table is 806 KB. The program accepts either a triplet of L*a*b* values , or an array of them, and calculates the MLab values for all inputs. The program's size is under 80 KB and it takes less than 1 second to convert a 512 by 512 array of L*a*b* to MLab.

The second set of LUTs makes the inverse estimation. It reads in MLab data and puts out L*a*b*. The **MLabtoLab** calculation has roughly the same sizes and speeds.

This means that anyone concerned with working in a truly uniform color space can do so by taking advantage of 3-D LUT technology. It takes only a second to get there.

Gabriel Marcu presented a recent paper using the same approach[15]. He used a 3-D LUT to convert L*a*b* to Mlab. He optimized portions of an out-of-gamut image in Mlab space. He got improved picture by interpolating in Mlab space.

We are very fortunate these days to have such a wide variety of reliable colorimetric equipment. Many of these devices provide direct L*a*b* measurements of high accuracy and reliability. The problem is not the devices, but the L*a*b* space, as seen above. In the future we can speculate that these devices will include MLab LUTs. Until then pairs of efficient 3-D LUT computer programs can easily transform our data into and out of the uniform Munsell color space.

WHEN DO WE CARE ?

Any time that you need to compare two colors and want to express that information as a distance you are implying that you are in an isotropic color space. It must conform to human appearance experiments in order to be isotropic. Using MLab instead of CIE L*a*b* will take you a big step toward being in an isotropic color space.

ACKNOWLEDGEMENTS

The author wishes to thank Gary Dispoto and Mike McGuire for their work on the very fast 3-D LUT running on Windows. I want to thank John Meyer, Gabrial Marcu and Mary McCann for their thoughtful discusions and comments.

[1]G. Wyszecki and W. S. Stiles, *Color Science: Concepts and Methods, Quantitative Data and Formulae*, Second edition, John Wiley & Sons, pp.852-861, (1982).

[2] E.H. Land and J. J. McCann, "Lightness and Retinex Theory, "*J. Opt. Soc. Am.* **61**, p. 1, 1971.

[3]D. Nickerson, ISCC Newsletter, No. **156**, Nov-Dec 1961.

[4]-M.D. Fairchild, "Color Appearance Models", Addison Wesley, p. 221, (1998).

[5] M.D. Fairchild, "Refinement of the RLAB Color Space", *Col. Res. & Appl.*, **21**, No. 5, pp. 338-346, (1996);
Ebner, F. and Fairchild, M.D, Gamut Mapping: Evaluation of Chroma Clipping Techniques for Three Destination Gamuts, *Proceedings of the 6th IS&T/SID Color Imaging Conference*, Scottsdale,Arizona, p. 57, (1998).

[6]S. M. Newhall, D. Nickerson and D. B Judd, Final report of the O.S.A. subcommittee on spacing of the Munsell colors, J. opt. Soc. Am, **33**,385.(1943).

[7] G. Wyszecki and W. S. Stiles, *Color Science: Concepts and Methods, Quantitative Data and Formulae*, Second edition, John Wiley & Sons, pp.840-852, (1982).

[8]D.L. MacAdam, Maximum Visual efficency of colored materials, J. opt. Soc. Am, 25,361 (1935).

[9]P.Hung and R.S.Berns, Determination of Constant Hue Loci for a CRT Gamut and Their Predictions Using Color Appearance Spaces, *Color Research and Application*, Vol. **20**, No.5, pp. 285-295, (1995); F. Ebner, and M.D., Finding Constant Hue Surfaces in Color Space, *Proceedings of SPIE, Color Imaging: Device-Independent Color, Color Hardcopy, and Graphic Arts III*, 3300-16, pp.107-117, (1998).

[10]P. Glatz and E, Luebbe, Colour Gamut Transformation Using Visually Assessed Colour Difference Folmula, Proc AIC, Kyoto, Vol. 1 p. 586, 1997; CIE, Technical Report, CIE No. **116** (1995); Braun and Fairchild, Color Gamut Mapping in a Hue -linearized CIELAB Color Space in *Proceedings of the 6th IS&T/SID Color Imaging Conference*, Scottsdale,Arizona, p. 163, (1998).

[11] M.D. Fairchild, "Refinement of the RLAB Color Space", *Col. Res. & Appl.*, **21**, No. 5, pp. 338-346, (1996)

[12]M. Abdulwahab, J. L. Burkhardt and J. J. McCann, Method and Apparatus for Transforming Color Image Data on the Basis of an Isotropic and Uniform Colorimetric Space, U. S. Patent, 4,839,721, Jun.13,1989.

[13]K.Kanamori, H.Kawakami, and H.Kotera:"A Novel Color Transformation Algorithm and Its Applications", Proc. SPIE., vol.1244,p.272-281(1990) ;
.K.Kanamori and H.Kotera:"Color Correction Technique for Hard Copies by 4-Neighbors Interpolation Method",Jour.Imag.Sci.&Tech., 36,1, p.73-80(1992); K.Kanamori, H.Kotera, O.Yamada, H.Motomura, R.Iikawa, T.Fumoto: "Fast Color Processor with Programmable Interpolation by Small Memory(PRISM)", Jour.Electronic Imaging, vol. 2(3), pp.213-224(1993);
H.Kotera,K.Kanamori,T.Fumoto,O.Yamada,H.Motomura and M.Inoue:"A Single Chip Color Processor for Device Independent Color Reproduction",Proc. 1 st CIC, p.133-137(1993);
T.Fumoto, K.Kanamori, O.Yamada, H.Motomura, and H.Kotera : "SLANT/PRISM Convertible Structured Color Processor MN5515, Proc. 3rd CIC, p.101-105(1995).

[14]J. J. McCann, High Resolution Color Photographic Reproductions, *Proc.of SPIE* , vol. **3025**, p 7, 1997.

[15]Gabriel Marcu, Gamut Mapping in Munsell Constant Hue Sections, in *Proceedings of the 6th IS&T/SID Color Imaging Conference*, Scottsdale,Arizona, p. 159, (1998).

Table1

Hue	Lightness	Chroma 2		4		6		8		10		12		14		16	
		Er	Er/C	Er	Er/C	Er	Er/C	Er	Er/C	Er	Er/C	Er	Er/C	Er	Er/C	Er	Er/C
2.5R	9	5.0	50%														
2.5R	8	4.4	44%	6.4	32%	8.8	29%										
2.5R	7	3.4	34%	6.1	30%	8.7	29%	11.3	28%								
2.5R	6	3.0	30%	5.5	27%	8.1	27%	11.0	27%	13.4	27%	15.7	26%				
2.5R	5	2.5	25%	4.7	24%	7.1	24%	9.5	24%	11.7	23%	13.6	23%	16.1	23%		
2.5R	4	2.1	21%	4.1	20%	6.1	20%	8.0	20%	10.0	20%	11.9	20%	13.4	19%		
2.5R	3	2.3	23%	3.8	19%	5.1	17%	6.6	16%	7.7	15%						
2.5R	2	0.7	7%	0.6	3%	2.3	8%	3.1	8%								
5.0R	9	4.2	42%														
5.0R	8	4.0	40%	5.5	28%	7.9	26%										
5.0R	7	2.9	29%	5.2	26%	7.5	25%	9.8	24%	12.2	24%						
5.0R	6	2.4	24%	4.6	23%	7.0	23%	9.5	24%	11.8	24%	14.0	23%				
5.0R	5	2.1	21%	4.0	20%	6.4	21%	8.7	22%	11.1	22%	13.2	22%	15.7	22%		
5.0R	4	1.9	19%	4.0	20%	6.0	20%	8.1	20%	10.3	21%	12.5	21%	14.5	21%		
5.0R	3	2.2	22%	3.7	19%	5.0	17%	6.7	17%	8.0	16%						
5.0R	2	0.7	7%	0.3	2%	1.9	6%	2.3	6%								
7.5R	9	3.6	36%														
7.5R	8	3.5	35%	4.7	23%	7.1	24%										
7.5R	7	2.4	24%	4.4	22%	6.7	22%	9.0	23%	11.6	23%						
7.5R	6	2.0	20%	4.0	20%	6.1	20%	8.6	21%	11.1	22%	13.9	23%				
7.5R	5	1.7	17%	3.4	17%	5.6	19%	8.1	20%	10.5	21%	13.0	22%	15.9	23%	19.0	24%
7.5R	4	1.4	14%	3.2	16%	5.0	17%	7.2	18%	9.4	19%	11.8	20%	14.5	21%	16.9	21%
7.5R	3	2.1	21%	3.5	17%	4.6	15%	6.5	16%	8.5	17%	9.9	16%				
7.5R	2	0.8	8%	0.3	1%	1.2	4%	1.6	4%								
10.0R	9	3.0	30%														
10.0R	8	2.9	29%	4.5	22%	7.3	24%										
10.0R	7	2.0	20%	4.3	21%	6.7	22%	9.5	24%	12.4	25%						
10.0R	6	1.7	17%	4.0	20%	6.4	21%	9.0	23%	12.5	25%	16.3	27%	21.0	30%		
10.0R	5	1.5	15%	3.7	18%	6.2	21%	9.2	23%	12.8	26%	17.0	28%	21.2	30%	27.5	34%
10.0R	4	1.6	16%	3.5	18%	5.5	18%	8.0	20%	11.0	22%	15.3	26%				
10.0R	3	2.1	21%	3.2	16%	4.4	15%	6.4	16%	8.9	18%	17.7	29%				
10.0R	2	0.9	9%	0.8	4%	0.3	1%										
2.5YR	9	2.4	24%	5.7	29%												
2.5YR	8	2.3	23%	5.0	25%	7.6	25%										
2.5YR	7	1.9	19%	4.3	22%	7.1	24%	9.9	25%	12.9	26%						
2.5YR	6	2.0	20%	4.2	21%	6.7	22%	9.4	23%	13.1	26%	17.8	30%	23.4	33%	30.1	38%
2.5YR	5	1.8	18%	3.8	19%	6.6	22%	10.0	25%	14.0	28%	18.7	31%	25.0	36%		
2.5YR	4	2.1	21%	4.2	21%	6.3	21%	9.4	24%	14.0	28%						
2.5YR	3	2.2	22%	3.6	18%	6.0	20%	9.4	24%								
2.5YR	2	1.0	10%	1.6	8%												
5.0YR	9	3.0	30%														
5.0YR	8	2.6	26%	5.8	29%	8.6	29%	12.7	32%								
5.0YR	7	2.4	24%	5.1	26%	8.3	28%	11.1	28%	14.9	30%	19.7	33%	25.2	36%	31.7	40%
5.0YR	6	2.4	24%	4.8	24%	8.1	27%	11.4	28%	15.1	30%	19.6	33%	25.0	36%		
5.0YR	5	2.2	22%	4.8	24%	8.1	27%	11.7	29%	15.2	30%	19.7	33%				
5.0YR	4	2.7	27%	5.3	27%	7.5	25%	10.5	26%								
5.0YR	3	2.4	24%	4.0	20%	7.0	23%										
5.0YR	2	1.1	11%	2.8	14%												
7.5YR	9	4.1	41%														
7.5YR	8	3.3	33%	6.5	33%	9.4	31%	13.4	33%								
7.5YR	7	3.0	30%	5.8	29%	9.1	30%	12.3	31%	16.8	34%						
7.5YR	6	2.9	29%	5.4	27%	8.8	29%	12.4	31%	16.1	32%	20.9	35%	26.1	37%		
7.5YR	5	2.5	25%	5.4	27%	9.1	30%	12.7	32%	16.6	33%	20.9	35%	26.0	37%		
7.5YR	4	3.1	31%	6.3	31%	8.5	28%	11.7	29%	16.3	33%						
7.5YR	3	2.6	26%	4.7	23%	7.9	26%										

Hue																	Table1	
Lightness								Chroma										
		2		4		6		8		10		12		14		16		
		Er	Er/C	Er	Er/C	Er	Er/C	Er	Er/C	Er	Er/C	Er	Er/C	Er	Er/C	Er	Er/C	
7.5YR	2	1.4	14%	4.1	21%													
10.0YR	9	5.6	56%	9.9	50%													
10.0YR	8	4.6	46%	8.0	40%	11.4	38%	15.2	38%	18.3	37%	22.3	37%	26.8	38%			
10.0YR	7	4.2	42%	7.7	38%	11.1	37%	14.3	36%	17.8	36%	22.4	37%	27.1	39%			
10.0YR	6	3.9	39%	7.1	35%	10.8	36%			18.2	36%	22.1	37%					
10.0YR	5	3.4	34%	6.9	35%	11.0	37%	14.4	36%	18.0	36%							
10.0YR	4	4.0	40%	7.4	37%	9.9	33%	13.1	33%									
10.0YR	3	2.9	29%	5.4	27%	9.2	31%											
10.0YR	2	1.7	17%															
2.5Y	9	6.6	66%	11.2	56%													
2.5Y	8	5.8	58%	9.3	47%	13.1	44%	16.4	41%	19.9	40%	24.1	40%	28.2	40%	32.2	40%	
2.5Y	7	5.3	53%	8.8	44%	12.4	41%	16.0	40%	20.1	40%	24.1	40%					
2.5Y	6	4.9	49%	8.4	42%	12.6	42%	16.5	41%	20.2	40%							
2.5Y	5	4.1	41%	8.3	41%	12.9	43%	16.0	40%									
2.5Y	4	4.5	45%	8.3	42%	11.2	37%											
2.5Y	3	3.2	32%	6.2	31%													
2.5Y	2	2.2	22%															
5.0Y	9	7.4	74%	12.4	62%	16.7	56%											
5.0Y	8	6.5	65%	10.9	54%	15.0	50%	18.9	47%	22.8	46%	27.3	45%	31.2	45%			
5.0Y	7	5.8	58%	10.3	52%	14.4	48%	18.0	45%	22.7	45%	26.3	44%	29.4	42%			
5.0Y	6	5.5	55%	9.7	48%	14.3	48%	18.5	46%			24.5	41%					
5.0Y	5	4.8	48%	9.5	47%	14.3	48%	17.5	44%	21.1	42%							
5.0Y	4	4.8	48%	9.2	46%	12.5	42%											
5.0Y	3	3.3	33%	6.7	34%													
5.0Y	2	2.1	21%															
7.5Y	9	7.9	79%	12.7	64%	17.1	57%											
7.5Y	8	6.9	69%	11.1	55%	15.4	51%	19.8	49%	23.9	48%	28.6	48%					
7.5Y	7	5.9	59%	10.6	53%	14.8	49%	19.1	48%	24.2	48%	27.7	46%					
7.5Y	6	5.7	57%	10.0	50%	15.3	51%	20.0	50%	23.6	47%							
7.5Y	5	4.8	48%	9.9	50%	15.3	51%	19.1	48%									
7.5Y	4	4.8	48%	9.7	49%	13.5	45%											
7.5Y	3	3.3	33%	7.1	35%													
7.5Y	2	1.8	18%															
10.0Y	9	8.1	81%	13.0	65%	17.5	58%											
10.0Y	8	7.1	71%	11.3	57%	15.9	53%	20.3	51%	24.9	50%	30.1	50%					
10.0Y	7	6.1	61%	10.8	54%	15.0	50%	19.9	50%	25.8	52%	29.7	49%					
10.0Y	6	5.7	57%	10.2	51%	15.4	51%	20.7	52%									
10.0Y	5	4.7	47%	10.1	50%	15.4	51%											
10.0Y	4	4.6	46%	9.8	49%	14.2	47%											
10.0Y	3	3.1	31%	7.4	37%													
10.0Y	2	1.2	12%															
2.5GY	9	8.2	82%	13.3	67%	17.8	59%											
2.5GY	8	7.2	72%	11.1	56%	15.6	52%	19.8	49%	25.4	51%	30.9	51%					
2.5GY	7	6.0	60%	10.5	52%	14.3	48%	19.3	48%	25.6	51%	30.3	51%					
2.5GY	6	5.5	55%	9.8	49%	14.6	49%	20.4	51%	24.9	50%							
2.5GY	5	4.3	43%	9.0	45%	14.3	48%	19.5	49%									
2.5GY	4	3.9	39%	9.1	46%	13.3	44%											
2.5GY	3	2.6	26%	7.0	35%													
2.5GY	2	0.5	5%															
5.0GY	9	8.1	81%	13.4	67%													
5.0GY	8	6.8	68%	10.8	54%	15.0	50%	18.9	47%	23.9	48%							
5.0GY	7	5.8	58%	9.8	49%	13.3	44%	17.7	44%	23.4	47%	28.9	48%					
5.0GY	6	5.2	52%	9.0	45%	13.1	44%	18.3	46%	23.4	47%							
5.0GY	5	3.8	38%	7.8	39%	12.5	42%	17.3	43%	22.3	45%							
5.0GY	4	3.3	33%	7.9	40%	11.8	39%	17.0	42%									

Table1

Hue	Lightness	Chroma 2		4		6		8		10		12		14		16	
		Er	Er/C	Er	Er/C	Er	Er/C	Er	Er/C	Er	Er/C	Er	Er/C	Er	Er/C	Er	Er/C
5.0GY	3	2.0	20%	5.6	28%	9.5	32%										
5.0GY	2	0.4	4%														
7.5GY	9	7.2	72%	11.2	56%												
7.5GY	8	5.8	58%	9.1	46%	12.3	41%	15.2	38%	18.7	37%						
7.5GY	7	4.9	49%	7.7	39%	10.4	35%	13.5	34%	17.5	35%						
7.5GY	6	4.4	44%	7.1	36%	10.0	33%	14.0	35%	17.6	35%	21.2	35%				
7.5GY	5	2.9	29%	5.8	29%	9.3	31%	12.6	32%	17.0	34%	15.4	26%				
7.5GY	4	2.2	22%	5.8	29%	9.2	31%	13.1	33%								
7.5GY	3	1.1	11%	3.8	19%	6.3	21%										
7.5GY	2	1.4	14%	1.5	8%												
10.0GY	9	6.2	62%	9.4	47%												
10.0GY	8	5.1	51%	7.5	38%	10.1	34%	11.5	29%								
10.0GY	7	4.1	41%	6.4	32%	7.9	26%	10.2	26%	12.6	25%						
10.0GY	6	3.6	36%	5.7	28%	7.8	26%	10.4	26%	12.4	25%						
10.0GY	5	2.3	23%	4.3	22%	6.7	22%	9.4	23%	12.0	24%						
10.0GY	4	1.6	16%	4.3	21%	7.2	24%	9.7	24%								
10.0GY	3	0.7	7%	2.6	13%	4.3	14%	6.2	15%								
10.0GY	2	1.8	18%	1.6	8%												
2.5G	9	5.2	52%	7.5	37%												
2.5G	8	4.2	42%	5.6	28%	8.0	27%	8.6	22%								
2.5G	7	3.3	33%	4.8	24%	5.6	19%	7.1	18%	8.7	17%						
2.5G	6	3.0	30%	4.5	23%	5.7	19%	6.9	17%	8.4	17%						
2.5G	5	1.8	18%	3.2	16%	4.7	16%	6.8	17%	8.5	17%	11.4	19%				
2.5G	4	1.2	12%	3.1	16%	5.7	19%	7.8	19%	10.4	21%						
2.5G	3	0.7	7%	2.3	11%	4.1	14%	5.7	14%	8.4	17%						
2.5G	2	2.1	21%	2.5	13%												
5.0G	9	4.3	43%														
5.0G	8	3.4	34%	4.3	21%	6.0	20%										
5.0G	7	2.6	26%	3.6	18%	3.9	13%	4.6	12%	6.0	12%						
5.0G	6	2.2	22%	3.7	18%	4.2	14%	4.9	12%	5.8	12%						
5.0G	5	1.2	12%	2.4	12%	3.4	11%	5.2	13%	6.7	13%						
5.0G	4	0.7	7%	2.3	12%	4.0	13%	5.9	15%	8.2	16%						
5.0G	3	0.6	6%	1.6	8%	2.9	10%	4.4	11%								
5.0G	2	2.1	21%	2.2	11%	3.4	11%										
7.5G	9	3.8	38%														
7.5G	8	3.0	30%	3.8	19%	4.9	16%										
7.5G	7	2.3	23%	3.0	15%	2.9	10%	3.1	8%								
7.5G	6	1.8	18%	3.1	16%	3.0	10%	3.1	8%	3.2	6%						
7.5G	5	1.0	10%	1.7	9%	2.0	7%	3.3	8%	3.8	8%						
7.5G	4	0.3	3%	1.6	8%	2.8	9%	3.6	9%	4.9	10%						
7.5G	3	0.6	6%	0.7	3%	1.3	4%	2.1	5%								
7.5G	2	2.2	22%	2.1	10%	2.7	9%										
10.0G	9	3.5	35%														
10.0G	8	2.7	27%	3.6	18%	4.6	15%										
10.0G	7	2.1	21%	2.8	14%	3.3	11%	3.7	9%								
10.0G	6	1.5	15%	2.9	15%	2.9	10%	3.2	8%	3.5	7%						
10.0G	5	0.9	9%	1.7	8%	1.8	6%	2.7	7%	2.8	6%						
10.0G	4	0.7	7%	1.5	7%	2.1	7%	2.4	6%	2.8	6%						
10.0G	3	0.8	8%	0.6	3%	0.4	1%	0.8	2%								
10.0G	2	2.3	23%	2.3	11%	3.1	10%										
2.5BG	9	3.6	36%														
2.5BG	8	2.9	29%	4.3	21%	5.5	18%										
2.5BG	7	2.3	23%	3.4	17%	4.4	15%	5.5	14%								
2.5BG	6	1.7	17%	3.3	16%	3.9	13%	4.6	11%	5.0	10%						
2.5BG	5	1.2	12%	2.2	11%	3.0	10%	3.6	9%	4.1	8%						

Hue																	Table1
Lightness								Chroma									
		2		4		6		8		10		12		14		16	
		Er	Er/C	Er	Er/C	Er	Er/C	Er	Er/C	Er	Er/C	Er	Er/C	Er	Er/C	Er	Er/C
2.5BG	4	0.9	9%	1.5	8%	2.0	7%	2.6	6%								
2.5BG	3	1.2	12%	1.0	5%	1.4	5%	2.1	5%								
2.5BG	2	2.4	24%	2.8	14%	3.9	13%										
5.0BG	9	3.2	32%														
5.0BG	8	2.6	26%	4.3	21%												
5.0BG	7	2.1	21%	3.4	17%	4.6	15%	5.8	15%								
5.0BG	6	1.6	16%	2.8	14%	3.6	12%	4.5	11%	5.5	11%						
5.0BG	5	1.0	10%	2.0	10%	3.0	10%	3.4	8%	3.8	8%						
5.0BG	4	0.9	9%	1.3	7%	1.7	6%	2.1	5%								
5.0BG	3	1.1	11%	0.9	4%	2.0	7%	2.5	6%								
5.0BG	2	2.4	24%	3.2	16%	4.7	16%										
7.5BG	9	2.6	26%														
7.5BG	8	2.1	21%	4.1	20%												
7.5BG	7	2.0	20%	3.5	18%	5.1	17%	6.6	16%								
7.5BG	6	1.5	15%	2.8	14%	4.0	13%	5.4	13%								
7.5BG	5	1.1	11%	2.4	12%	3.6	12%	4.3	11%								
7.5BG	4	1.0	10%	1.6	8%	2.1	7%	2.7	7%								
7.5BG	3	1.1	11%	1.0	5%	2.2	7%	3.4	8%								
7.5BG	2	2.3	23%	3.4	17%	4.8	16%										
10.0BG	9	2.6	26%														
10.0BG	8	2.2	22%	4.2	21%												
10.0BG	7	1.9	19%	3.5	18%	5.3	18%	6.6	16%								
10.0BG	6	1.6	16%	2.8	14%	3.9	13%	5.4	13%								
10.0BG	5	1.2	12%	2.4	12%	3.3	11%	4.2	11%	5.0	10%						
10.0BG	4	1.0	10%	1.6	8%	2.4	8%	2.9	7%								
10.0BG	3	0.9	9%	1.3	6%	2.5	8%	3.9	10%								
10.0BG	2	2.2	22%	3.5	18%	5.1	17%										
2.5B	9	2.3	23%														
2.5B	8	2.5	25%	4.3	22%												
2.5B	7	2.1	21%	3.7	18%	5.4	18%	6.9	17%								
2.5B	6	1.9	19%	3.3	17%	4.3	14%	5.5	14%								
2.5B	5	1.5	15%	2.7	13%	3.8	13%	4.9	12%	5.7	11%						
2.5B	4	1.2	12%	1.7	9%	3.1	10%	3.6	9%								
2.5B	3	0.8	8%	1.3	6%	2.8	9%	4.2	11%								
2.5B	2	2.0	20%	3.4	17%	5.0	17%										
5.0B	9	2.7	27%														
5.0B	8	2.8	28%	4.0	20%												
5.0B	7	2.3	23%	3.8	19%	5.3	18%	6.7	17%								
5.0B	6	2.2	22%	3.7	18%	4.6	15%	5.8	14%	7.5	15%						
5.0B	5	1.7	17%	3.1	15%	4.3	14%	5.6	14%	7.3	15%						
				2.1	11%	3.9	13%	5.0	13%	6.8	14%						
5.0B	3	0.7	7%	1.5	8%	3.7	12%	5.8	14%								
5.0B	2	1.8	18%	3.4	17%	5.5	18%	7.3	18%								
7.5B	9	3.3	33%														
7.5B	8	3.3	33%	4.6	23%												
7.5B	7	2.8	28%	4.5	22%	6.1	20%	7.3	18%								
7.5B	6	2.5	25%	4.2	21%	5.4	18%	7.1	18%	9.1	18%						
7.5B	5	2.0	20%	3.4	17%	5.1	17%	7.0	18%	9.2	18%						
7.5B	4	1.4	14%	2.7	13%	4.9	16%	6.6	17%	9.4	19%						
7.5B	3	0.6	6%	2.0	10%	4.5	15%	7.0	17%								
7.5B	2	1.5	15%	3.6	18%	6.1	20%										
10.0B	9	3.8	38%														
10.0B	8	3.6	36%	4.8	24%	5.9	20%										
10.0B	7	3.2	32%	5.0	25%	6.8	23%	8.2	21%								
10.0B	6	2.7	27%	4.8	24%	6.2	21%	8.1	20%	10.3	21%						

Table1

Hue	Lightness	Chroma 2		4		6		8		10		12		14		16	
		Er	Er/C	Er	Er/C	Er	Er/C	Er	Er/C	Er	Er/C	Er	Er/C	Er	Er/C	Er	Er/C
10.0B	5	2.1	21%	3.9	19%	5.9	20%	7.9	20%	10.1	20%	12.2	20%				
10.0B	4	1.6	16%	3.1	16%	5.5	18%	7.4	19%	10.2	20%						
10.0B	3	0.7	7%	2.4	12%	4.9	16%	7.4	18%	10.3	21%						
10.0B	2	1.5	15%	3.7	18%	6.0	20%										
2.5PB	9	4.2	42%														
2.5PB	8	3.9	39%	5.2	26%	6.2	21%										
2.5PB	7	3.5	35%	5.3	27%	7.3	24%	9.0	22%								
2.5PB	6	3.0	30%	5.3	26%	6.9	23%	9.1	23%	11.4	23%						
2.5PB	5	2.3	23%	4.4	22%	6.3	21%	8.8	22%	11.4	23%	14.0	23%				
2.5PB	4	3.5	35%	6.7	34%	9.7	32%	12.2	31%	14.9	30%						
2.5PB	3	1.1	11%	3.0	15%	5.6	19%	8.7	22%								
2.5PB	2	1.6	16%	4.0	20%	6.9	23%										
5.0PB	9	4.4	44%														
5.0PB	8	4.1	41%	5.5	27%	6.1	20%										
5.0PB	7	3.6	36%	5.6	28%	7.4	25%	9.1	23%								
5.0PB	6	3.1	31%	5.5	27%	7.0	23%	9.3	23%	11.7	23%						
5.0PB	5	2.4	24%	4.7	23%	6.7	22%	9.0	23%	11.6	23%	14.2	24%				
5.0PB	4	1.8	18%	4.0	20%	6.3	21%	8.6	21%	11.6	23%	15.1	25%				
5.0PB	3	1.6	16%	3.5	17%	5.8	19%	8.9	22%	12.3	25%						
5.0PB	2	1.9	19%	4.2	21%	7.0	23%	10.5	26%								
7.5PB	9	4.6	46%														
7.5PB	8	4.3	43%	5.7	29%												
7.5PB	7	3.7	37%	5.8	29%	7.7	26%	9.7	24%								
7.5PB	6	3.1	31%	5.5	28%	7.6	25%	10.6	27%	13.6	27%						
7.5PB	5	2.5	25%	4.9	25%	7.3	24%	10.5	26%	13.9	28%						
7.5PB	4	2.1	21%	4.7	23%	7.6	25%	10.9	27%	14.5	29%	18.6	31%				
7.5PB	3	2.5	25%	5.0	25%	8.3	28%	12.2	30%	16.6	33%	21.9	37%				
7.5PB	2	2.6	26%	5.6	28%	9.6	32%	14.3	36%	20.2	40%						
10.0PB	9	4.7	47%														
10.0PB	8	4.4	44%	9.1	46%												
10.0PB	7	3.6	36%	5.5	28%	7.8	26%	10.1	25%								
10.0PB	6	3.0	30%	5.4	27%	7.7	26%	10.8	27%	13.9	28%						
10.0PB	5	2.5	25%	5.0	25%	7.6	25%	10.8	27%	14.5	29%						
10.0PB	4	2.3	23%	5.0	25%	8.1	27%	11.6	29%	15.3	31%	19.6	33%				
10.0PB	3	3.1	31%	5.8	29%	9.2	31%	13.1	33%	17.6	35%						
10.0PB	2	3.2	32%	6.3	32%	10.2	34%	14.7	37%	19.9	40%						
2.5P	9	4.4	44%	5.0	25%												
2.5P	8	4.4	44%	5.7	28%												
2.5P	7	3.4	34%	5.5	28%	7.9	26%	10.2	26%								
2.5P	6	2.8	28%	5.3	27%	7.5	25%	10.3	26%	13.4	27%						
2.5P	5	2.4	24%	4.7	23%	7.3	24%	10.4	26%	13.9	28%						
2.5P	4	2.2	22%	4.7	23%	7.6	25%	11.0	28%	14.8	30%	18.7	31%				
2.5P	3	3.2	32%	5.7	28%	8.7	29%	12.3	31%	16.5	33%						
2.5P	2	3.1	31%	5.8	29%	9.4	31%	13.7	34%	18.1	36%						
5P	9	4.6	46%	4.4	22%												
5.0P	8	4.5	45%	5.6	28%												
5.0P	7	3.4	34%	5.5	27%	7.6	25%	9.9	25%								
5.0P	6	2.6	26%	5.1	25%	7.2	24%	9.9	25%								
5.0P	5	2.4	24%	4.6	23%	6.9	23%	9.6	24%	12.6	25%						
5.0P	4	2.0	20%	4.2	21%	6.8	23%	9.7	24%	12.8	26%	16.2	27%				
5.0P	3	3.1	31%	5.1	26%	7.5	25%	10.5	26%	13.8	28%						
5.0P	2	2.8	28%	5.0	25%	8.0	27%	11.3	28%								
7.5P	9	5.2	52%	6.5	33%												
7.5P	8	5.0	50%	6.9	34%	9.6	32%										
7.5P	7	4.0	40%	6.5	32%	9.0	30%	11.4	29%								

Hue																Table1	
Lightness		Chroma															
		2		4		6		8		10		12		14		16	
		Er	Er/C	Er	Er/C	Er	Er/C	Er	Er/C	Er	Er/C	Er	Er/C	Er	Er/C	Er	Er/C
7.5P	6	3.0	30%	6.0	30%	8.0	27%	10.8	27%	13.2	26%						
7.5P	5	2.7	27%	5.0	25%	7.3	24%	9.7	24%	12.6	25%						
7.5P	4	2.0	20%	4.1	20%	6.5	22%	9.1	23%	11.8	24%	14.5	24%				
7.5P	3	2.9	29%	4.5	22%	6.4	21%	8.7	22%	11.1	22%						
7.5P	2	2.4	24%	3.9	20%	6.2	21%										
10.0P	9	5.3	53%														
10.0P	8	5.1	51%	7.2	36%	9.5	32%										
10.0P	7	4.0	40%	6.7	33%	9.1	30%	11.4	28%								
10.0P	6	3.2	32%	5.9	30%	8.1	27%	10.8	27%	13.2	26%						
10.0P	5	2.8	28%	5.2	26%	7.4	25%	9.5	24%	12.1	24%	14.4	24%				
10.0P	4	2.0	20%	4.0	20%	6.1	20%	8.3	21%	10.7	21%	13.1	22%				
10.0P	3	2.5	25%	3.8	19%	5.2	17%	6.9	17%	8.6	17%						
10.0P	2	2.0	20%	2.9	14%	4.6	15%										
2.5RP	9	5.3	53%														
2.5RP	8	5.1	51%	7.6	38%	10.1	34%										
2.5RP	7	4.1	41%	7.1	35%	9.3	31%	11.8	30%	14.7	29%						
2.5RP	6	3.3	33%	6.3	32%	8.6	29%	11.5	29%	14.1	28%	16.3	27%				
2.5RP	5	2.9	29%	5.4	27%	7.5	25%	9.5	24%	12.2	24%	14.4	24%				
2.5RP	4	2.1	21%	4.2	21%	6.2	21%	8.4	21%	10.7	21%	12.8	21%				
2.5RP	3	2.3	23%	3.8	19%	5.3	18%	6.9	17%	8.5	17%						
2.5RP	2	2.0	20%	2.6	13%	4.4	15%	5.3	13%								
5.0RP	9	5.3	53%														
5.0RP	8	5.2	52%	8.0	40%	10.8	36%										
5.0RP	7	4.3	43%	7.6	38%	10.4	35%	13.3	33%	16.6	33%	19.0	32%				
5.0RP	6	3.7	37%	6.9	35%	9.6	32%	12.7	32%	15.9	32%	18.5	31%				
5.0RP	5	3.3	33%	6.1	30%	8.7	29%	11.2	28%	14.0	28%	16.4	27%				
5.0RP	4	2.5	25%	4.9	24%	7.2	24%	9.4	24%	12.1	24%						
5.0RP	3	2.4	24%	4.1	20%	5.6	19%	7.0	18%	8.4	17%						
5.0RP	2	1.7	17%	2.3	11%	3.8	13%	4.4	11%								
7.5RP	9	5.2	52%														
7.5RP	8	5.0	50%	7.7	38%	10.3	34%										
7.5RP	7	4.1	41%	7.4	37%	10.1	34%	12.9	32%								
7.5RP	6	3.6	36%	6.7	34%	9.3	31%	12.6	32%	15.4	31%	17.9	30%				
7.5RP	5	3.2	32%	6.0	30%	8.6	29%	10.9	27%	13.7	27%	15.6	26%	18.3	26%		
7.5RP	4	2.5	25%	5.0	25%	7.3	24%	9.5	24%	11.9	24%	13.8	23%				
7.5RP	3	2.4	24%	4.0	20%	5.4	18%	6.7	17%	8.1	16%						
7.5RP	2	1.2	12%	1.5	7%	3.1	10%	3.7	9%							ALL	H&C
10.0RP	9	5.0	50%													8.1	42%
10.0RP	8	4.8	48%	7.2	36%	9.9	33%									17.7	38%
10.0RP	7	3.9	39%	6.8	34%	9.7	32%	12.6	31%							15.4	32%
10.0RP	6	3.4	34%	6.3	31%	8.9	30%	12.1	30%	14.7	29%	17.2	29%			13.8	29%
10.0RP	5	3.0	30%	5.6	28%	8.1	27%	10.5	26%	13.0	26%	14.9	25%	17.6	25%	11.8	25%
10.0RP	4	2.3	23%	4.6	23%	6.8	23%	8.9	22%	11.2	22%	13.0	22%	14.8	21%	9.8	22%
10.0RP	3	2.4	24%	4.0	20%	5.5	18%	6.9	17%	8.2	16%					7.5	21%
10.0RP	2	0.8	8%	0.9	4%	2.6	9%	3.5	9%							6.5	20%
All		7.6	27%					Averages									
All	L	3.0	30%	5.1	26%	7.3	24%	9.5	24%	13.2	26%	18.5	31%	21.7	31%	26.2	33%
	9	4.7	47%	7.8	39%	11.6	39%										
	8	4.2	41%	6.4	32%	8.8	29%	11.6	29%	22.2	44%	27.2	45%	28.7	41%	32.2	40%
	7	3.5	34%	5.9	29%	8.0	27%	10.5	26%	13.7	27%	22.5	38%	27.2	39%	31.7	40%
	6	3.1	29%	5.3	27%	7.7	26%	10.3	26%	12.5	25%	17.2	29%	23.9	34%	30.1	38%
	5	2.5	24%	4.7	24%	7.3	24%	9.5	24%	12.6	25%	15.7	26%	19.0	27%	23.2	29%
	4	2.2	21%	4.4	22%	6.7	22%	8.3	21%	11.1	22%	14.4	24%	14.5	21%	16.9	21%
	3	1.9	22%	4.1	21%	5.7	19%	7.4	18%	10.2	20%	16.0	27%				
	2	1.7	22%	2.6	13%	4.0	13%	5.2	13%	19.0	38%						